

SCIENTIFIC REPORTS



OPEN

Rydberg interaction induced enhanced excitation in thermal atomic vapor

Dushmanta Kara, Arup Bhowmick & Ashok K. Mohapatra

We present the experimental demonstration of interaction induced enhancement in Rydberg excitation or Rydberg anti-blockade in thermal atomic vapor. We have used optical heterodyne detection technique to measure Rydberg population due to two-photon excitation to the Rydberg state. The anti-blockade peak which doesn't satisfy the two-photon resonant condition is observed along with the usual two-photon resonant peak which can't be explained using the model with non-interacting three-level atomic system. A model involving two interacting atoms is formulated for thermal atomic vapor using the dressed states of three-level atomic system to explain the experimental observations. A non-linear dependence of vapor density is observed for the anti-blockade peak which also increases with increase in principal quantum number of the Rydberg state. A good agreement is found between the experimental observations and the proposed interacting model. Our result implies possible applications towards quantum logic gates using Rydberg anti-blockade in thermal atomic vapor.

Long range many body interaction in Rydberg atoms give rise to many interesting phenomena. The suppression in Rydberg population or the excitation blockade is the most striking one giving rise to a variety of applications¹. A highly dense atomic ensemble behaves like a single super atom producing a strongly correlated many body system² and also leading to a single photon source³. The phenomenon has been experimentally observed in an atomic ensemble in a magneto optical trap⁴⁻⁷, in a magnetic trap^{8,9} and also in a single atom trap^{10,11}. Many theoretical models focus on the study of strongly correlated many body system in ultra cold atom and Bose Einstein condensate¹²⁻¹⁵. Rydberg blockade interaction can induce optical non-linearity which is non-local¹⁶ and also strong enough to observe for single photon^{17,18}. Rydberg blockade interaction may also lead to applications such as quantum gates using atoms¹⁹⁻²². An opposite effect of Rydberg blockade with enhancement in Rydberg excitation facilitated by interaction called as the Rydberg anti-blockade has been proposed in ultra cold atomic gas using a two photon excitation to Rydberg state²³. An experiment performed in ultra cold ensemble of atoms verifies the effect based on the theoretical model²⁴. It has been proposed that resonant dipole dipole interaction has non-additive character due to anti-blockade in an ensemble having more than two atoms in the blockade sphere²⁵. In addition to this, the existence of anti-blockade between two Rydberg atoms, interacting with a zero area phase jump pulse is also reported²⁶. Some recent results have also been reported to study Rydberg anti blockade in atomic²⁷⁻²⁹ and molecular resonances³⁰. The implementation of quantum logic gate using Rydberg anti-blockade has also recently been proposed³¹⁻³³.

Recent experiments with thermal vapor have drawn the attention to study Rydberg interaction induced many-body effects³⁴⁻³⁸. Electromagnetically induced transparency involving Rydberg state in thermal vapor cell as well as in micron size vapor cell has been studied^{39,40}. In addition, four wave mixing for a Rydberg state⁴¹ and Kerr non-linearity in Rydberg EIT has also been reported in thermal Rubidium vapor⁴². A recent study of Rydberg blockade in thermal atomic vapor has also been performed⁴³. Anomalous excitation facilitated by Rydberg interaction has also been proposed recently in thermal atomic vapor⁴⁴. In this article, we present a strong evidence of enhancement in Rydberg excitation due to interaction in thermal atomic vapor. An interacting twoatom model is formulated using the dressed state picture of a three level system in cold atomic ensemble. The model is further extended to thermal atomic vapor by Doppler averaging over the ensemble. An experiment has been performed in thermal rubidium vapor using optical heterodyne detection technique⁴⁵ to observe the anti-blockade effect. A good match is found between the model and the experimental observation as an evidence of the existence of

School of Physical Sciences, National Institute of Science Education and Research Bhubaneswar, HBNI, Jatni, 752050, India. Correspondence and requests for materials should be addressed to A.K.M. (email: a.mohapatra@niser.ac.in)

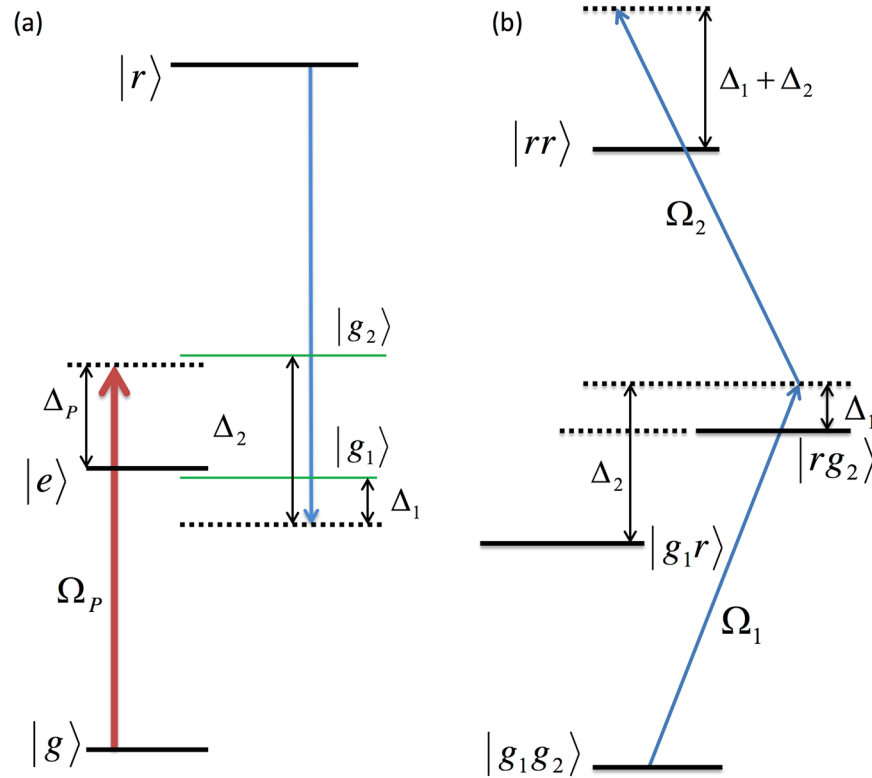


Figure 1. The relevant energy level diagrams. **(a)** A probe laser driving the $|g\rangle \rightarrow |e\rangle$ transition of a single atom leads to the dressed states $|g_1\rangle$ and $|g_2\rangle$. The coupling laser drives the dressed states to the Rydberg state $|r\rangle$ with detuning $\Delta_1 \simeq \Delta_C - \Omega_p^2/4\Delta_p$ and $\Delta_2 \simeq \Delta_p + \Delta_C + \Omega_p^2/4\Delta_p$ respectively. **(b)** The twoatom model with states $|g_1g_2\rangle$ representing an atom in each dressed states, $|g_1r\rangle$, $|rg_2\rangle$ representing one atom in the respective dressed state and other atom in the Rydberg state and $|rr\rangle$ representing both the atoms in the Rydberg state.

Rydberg anti-blockade in thermal atomic vapor. This is the first ever direct spectroscopic observation of Rydberg anti-blockade in thermal atomic vapor.

Results

Theoretical model. Let us consider a three level atomic system with states $|g\rangle$, $|e\rangle$ and $|r\rangle$ as shown in Fig. 1(a). The probe (coupling) laser drives the transition $|g\rangle \rightarrow |e\rangle$ ($|e\rangle \rightarrow |r\rangle$) with Rabi frequency Ω_p (Ω_C) and detuning Δ_p (Δ_C). Both of these transitions are dipoleallowed whereas the transition $|g\rangle \rightarrow |r\rangle$ is dipoleforbidden. The population decay rates of the transitions $|e\rangle \rightarrow |g\rangle$ and $|r\rangle \rightarrow |e\rangle$ are Γ_{eg} and Γ_{re} respectively. We have also included a decay rate Γ_{rg} to account for the indirect decay of the state $|r\rangle \rightarrow |g\rangle$ due to finite transit time of the thermal atoms. In the regime $\Omega_C \ll \Omega_p$, interaction with the coupling laser can be treated as a small perturbation to the atomic states dressed by the strong probe laser. For large probe detuning $\Delta_p \gg \Omega_p$ and Γ_{eg} , the dressed states are given by $|g_1\rangle \approx |e\rangle + \frac{\Omega_p}{2\Delta_p}|g\rangle$ and $|g_2\rangle \approx |g\rangle - \frac{\Omega_p}{2\Delta_p}|e\rangle$ with difference in their energy eigenvalues $\Delta \simeq \Delta_p + \Omega_p^2/2\Delta_p$. The steady state population of the dressed states can be determined by diagonalizing the steady state density matrix for the two-level atomic transition $|g\rangle \rightarrow |e\rangle$ driven by the strong probe laser. The population of the states $|g_1\rangle$ and $|g_2\rangle$ are found to be approximately $\Omega_p^4/16\Delta_p^4$ and 1 respectively. When the coupling laser is scanned over these dressed states, each of them will behave like a ground state exciting to the Rydberg state by the coupling laser. It is to be noted that the optical pumping rate to achieve the steady state population of the dressed states is Γ_{eg} . If $\Omega_C \ll \Gamma_{eg}$ then the coupling laser driving to the Rydberg state can not build the coherence between the dressed states. Hence, both the states can be treated independently and the total Rydberg population can be determined by adding the individual Rydberg populations driven from each of the dressed states. The coupling Rabi frequencies are scaled for each dressed state as $\Omega_1 \approx \Omega_C$ for the transition $|g_1\rangle \rightarrow |r\rangle$ and $\Omega_2 \approx \Omega_p\Omega_C/2\Delta_p$ for the transition $|g_2\rangle \rightarrow |r\rangle$. Similarly, the population of the Rydberg state will decay to the states $|g_1\rangle$ and $|g_2\rangle$ with decay rates as $\Gamma_1 \simeq \Gamma_{re} + \frac{\Omega_p}{2\Delta_p}\Gamma_{rg}$ and $\Gamma_2 \simeq \Gamma_{rg} + \frac{\Omega_p}{2\Delta_p}\Gamma_{re}$ respectively.

Considering two atoms driven to the Rydberg state simultaneously, there are four possible dressed states as $|g_1g_1\rangle$, $|g_2g_2\rangle$, $|g_1g_2\rangle$ and $|g_2g_1\rangle$. The states $|g_1g_2\rangle$ and $|g_2g_1\rangle$ are degenerate and have equal steady state population of $\Omega_p^4/16\Delta_p^4$. The population of the state $|g_2g_2\rangle$ is approximately 1 and that of $|g_1g_1\rangle$ is negligibly small for $\Omega_p \ll \Delta_p$. The difference in the energy eigenvalues of $|g_2g_2\rangle$ and $|g_1g_2\rangle$ is Δ which can be made larger than the typical Doppler linewidth of the transition in thermal vapor. If a narrow band laser is made resonant to the transition $|g_1g_2\rangle \rightarrow |rg_2\rangle$, then the laser will be out of resonance to drive the atoms in the state $|g_2g_2\rangle$ to the

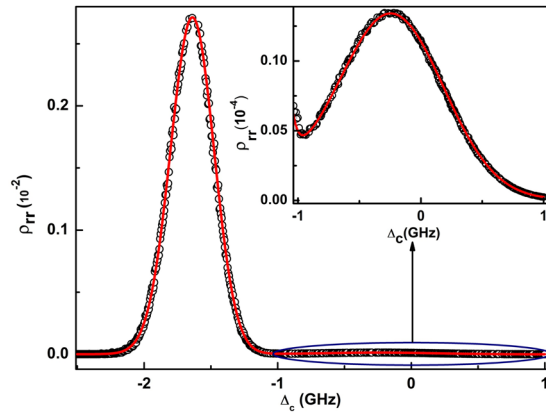


Figure 2. Rydberg population as a function of coupling laser detuning. Rydberg population calculated using exact three level single atomic system and two-atoms non-interacting model are represented by the solid line and the symbol ($^{\circ}$) respectively. Inset shows the magnified view of the peak near $\Delta_c=0$. Laser parameters used in the calculation are $\Omega_p=400$ MHz, $\Omega_c=5$ MHz and $\Delta_p=1.25$ GHz.

Rydberg state. In the regime $\Omega_c \ll \Gamma_{eg}$, the coupling laser can't introduce coherence between the states $|g_1 g_2\rangle$ and $|g_2 g_1\rangle$. Hence, either of the states can be considered in the two atom model to determine the Rydberg population with proper normalization accounting for both the states. Thus in the simplified model, only one of the dressed states of the two atomic system can be considered to model the anti-blockade peak. As shown in Fig. 1(b), the relevant energy level diagram to model the anti-blockade peak are $|g_1 g_2\rangle$, $|g_2 r\rangle$, $|r g_2\rangle$ and $|rr\rangle$. Steady state solutions of the master equation using the above simplified model and averaging over the thermal ensemble (see method section) is depicted in Fig. 2. In the regime $\Omega_c \ll \Gamma_{eg}$, the non-interacting two-atom dressed state model matches excellent with the exact three-level single atom calculation which tends to deviate with increase in Ω_c above Γ_{eg} . It can be shown that the $|g_2\rangle \rightarrow |r\rangle$ transition is equivalent to the effective two-level transition ($|g\rangle \rightarrow |r\rangle$) by adiabatically eliminating the intermediate state $|e\rangle$ of a three-level system⁴⁶. The Rydberg population due to the $|g_1\rangle \rightarrow |r\rangle$ transition which is neglected in the model with effective two-level system can be shown to be enhanced due to Rydberg-Rydberg interaction. Hence, the exact model for three-level system for two interacting atoms is necessary to study the anti-blockade peak. However, for the given laser parameters discussed above, the dressed state model is simplified due to reduced Hilbert space relevant for modelling the anti-blockade peak.

Rydberg-Rydberg interaction can easily be introduced in the model by including the shift in energy of the $|rr\rangle$ state. Rydberg anti-blockade in thermal vapor is illustrated in Fig. 3. Consider a case where the narrow band laser is resonant to the $|g_1 g_2\rangle \rightarrow |r g_2\rangle$ transition as depicted in Fig. 3(a). Then the atom in the dressed state $|g_1\rangle$ is excited to the Rydberg state. The same laser will be out of resonance to the $|g_1 g_2\rangle \rightarrow |g_1 r\rangle$ transition. If the Rydberg-Rydberg interaction is absent then the state $|rr\rangle$ will also not satisfy the resonant condition. Therefore, the second atom in the dressed state $|g_2\rangle$ can't be excited to the Rydberg state. Suppose the interaction shift of the $|rr\rangle$ state is equal to Δ' (difference in the resonant frequencies corresponding to the $|g_1 g_2\rangle \rightarrow |r g_2\rangle$ and $|g_1 g_2\rangle \rightarrow |g_1 r\rangle$ transitions) then the $|rr\rangle$ state will be resonant to the laser as shown in Fig. 3(a). Now the second atom present in the state $|g_2\rangle$ will also be excited to the Rydberg state unlike a non-interacting system. So the presence of the Rydberg interaction facilitate the excitation of the second atom enhancing the total Rydberg population compared to the non-interacting case and this phenomenon is known as Rydberg anti-blockade. Rydberg anti-blockade peak appears when the coupling laser is resonant to the $|g_1\rangle \rightarrow |r\rangle$ transition i.e. near $\Delta_c=0$, whereas the usual two-photon resonant peak appears with the coupling laser resonating to the $|g_2\rangle \rightarrow |r\rangle$ transition. Referring to Fig. 3(b), consider an interaction sphere with radius r_b where r_b is defined as the blockade radius and is given by $r_b = \sqrt[6]{\frac{C_6}{\hbar\Omega_2}}$, with C_6 being the coefficient of van der Waals interaction. Consider the atom in the dressed state $|g_1\rangle$ resonating to the coupling laser to be at the center of the sphere. Assume that the second atom in the dressed state $|g_2\rangle$ is present in a concentric spherical shell with radius $|r\rangle$ and thickness dr . Referring to Fig. 3(a), if $\Delta_1 + \Delta' = 2C_6/r^6$, then both the atoms will be excited to the $|rr\rangle$ state which will lead to the enhanced Rydberg excitation or anti-blockade. In a thermal atomic ensemble, effect of the atomic velocity distribution should be included in the detuning Δ_1 and also in Δ' . Hence, in thermal atomic vapor, not all but only a specific velocity class of atoms in the given spherical shell of radius $|r\rangle$ can satisfy the resonance condition to the $|rr\rangle$ state. Then, the Rydberg population due to anti-blockade can be evaluated by averaging over the velocity distribution of the thermal ensemble and integrating over the interaction sphere (see method section). It is to be noted that the motion of the atom due to Rydberg-Rydberg interaction (e.g. for $n=50$ state) is of the order of 100 nm while transiting through the laser beam of size 100 μm which can be neglected. In a regime $\Omega_p \gg \Omega_c$, the dispersion of the probe beam is shown to be proportional to the Rydberg population⁴⁵. So, the probe dispersion spectrum by changing the coupling laser detuning was calculated from the theoretical model which is shown in Fig. 3(c). However, the model will explain only the anti-blockade peak as the laser was resonant to the transition $|g_1 g_2\rangle \rightarrow |r g_2\rangle$. The usual two photon resonant peak can be determined by considering excitation from the ground state $|g_2 g_2\rangle$. For a comparison, the exact 3-level single atom calculation is also

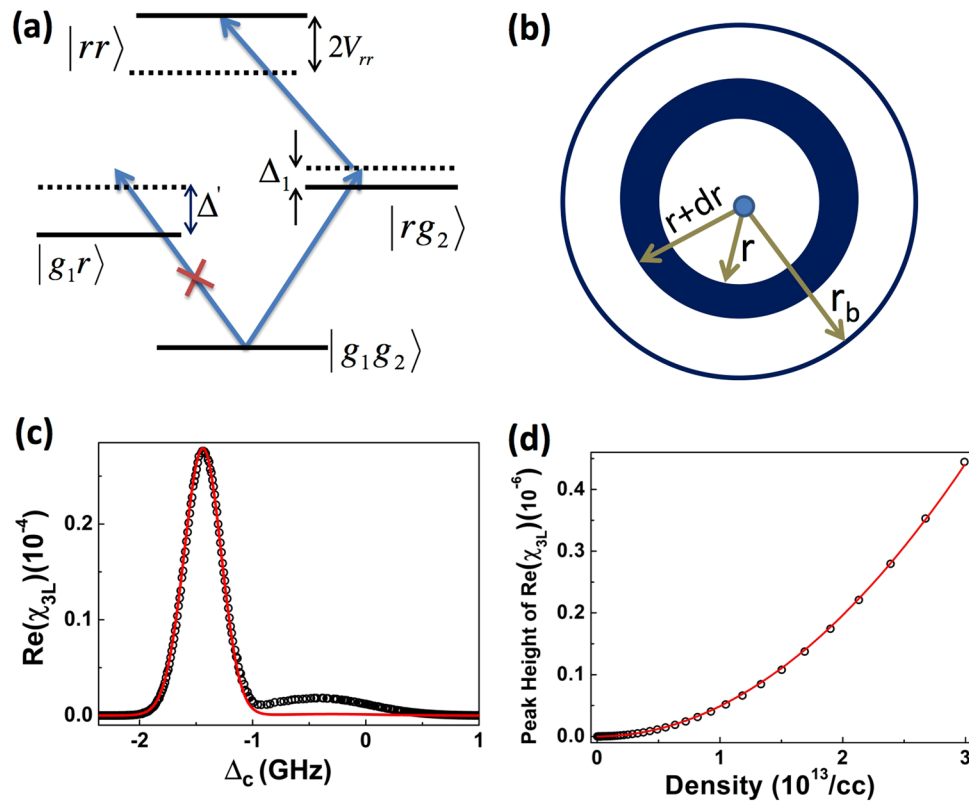


Figure 3. (a) Energy level diagram to model Rydberg anti-blockade. Δ_1 and Δ_2 ($=\Delta_1 + \Delta'$) are the coupling laser detuning of atom 1 and 2 respectively. (b) Schematic of the interaction sphere of radius r_b . The atom in the dressed state $|g_2\rangle$ is placed at the centre of the sphere. The atoms in the spherical shell of radius r and thickness dr can compensate for the two-photon resonance to the $|rr\rangle$ state due to van der Waals type Rydberg-Rydberg interaction ($V_{rr} = C_6/r^6$) with the atom at the center. (c) Dispersion spectrum of the probe laser calculated using non-interacting model (solid line) and two-atoms interacting model (black open circle). (d) Calculated dispersion peak height of the anti-blockade peak using two-atoms interacting model (black open circle) showing the quadratic dependence (solid line) of density.

depicted in the same figure. Anti-blockade peak is observed to be enhanced significantly due to interaction compared to the non-interacting case. Referring to eq. (1) in method section, the dispersion of the probe beam due to two atoms interaction depends strongly on the principal quantum number of the Rydberg state and also depends quadratically on the density of the atomic vapor. The dispersion peak height of the anti-blockade peak calculated from the interacting model showing a quadratic dependence on the density of the atomic vapor is depicted in Fig. 3(d).

Experimental results and discussions. Schematic of the experimental set up is depicted in Fig. 4(a). Optical heterodyne detection technique (OHDT)^{42,45} was used to measure the dispersion of the probe beam propagating through a magnetically shielded rubidium vapor cell. The details of the OHDT and the theoretical model for relating the dispersion with Rydberg population can be found in ref.⁴⁵. Optical heterodyne detection technique requires a probe laser beam along with a reference laser beam which were derived from an external cavity diode laser operating at 780 nm. A frequency offset of 800 MHz between the probe and the reference beams was introduced using acousto-optic modulators. The coupling laser beam operating in the range of 478 nm to 482 nm counter-propagates the probe beam through the vapor cell. The overlapping between the probe and coupling beam was ensured by optimizing the Rydberg EIT signal. The beam waist of the probe (coupling) laser was 95 μm (80 μm) and the respective Rayleigh range was 36.33 mm (41.86 mm). The probe laser power was kept fixed at 4 mW throughout the experiment. For the coupling laser the power was varied following the $n^{3/2}$ law, so as to keep the coupling Rabi frequency constant for all the n states. The Rabi frequencies of the probe and coupling beams were determined from their intensity using the method discussed in ref.⁴². The inhomogeneity of the laser intensity profile is neglected in the model and the averaged Rabi frequencies were used to compare with the experimental observation. The density of the vapor was varied by heating the cell and the temperature was controlled using a PID controller. The non-linear phase shift of the probe laser due to two-photon excitation to the Rydberg state in the presence of the coupling laser can be measured by comparing the phase of the reference beam using OHDT⁴⁵. A typical dispersion spectrum observed in the experiment is shown in Fig. 4(b).

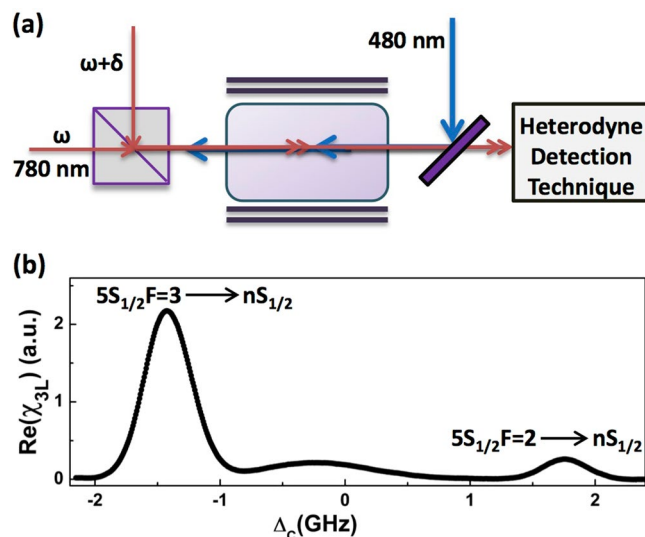


Figure 4. (a) Schematic of the experimental set up. (b) A typical dispersion spectrum of the probe laser observed using the optical heterodyne detection technique showing the resonant peaks corresponding to $5S_{1/2}F=3 \rightarrow nS_{1/2}$ and $5S_{1/2}F=2 \rightarrow nS_{1/2}$ of ^{85}Rb .

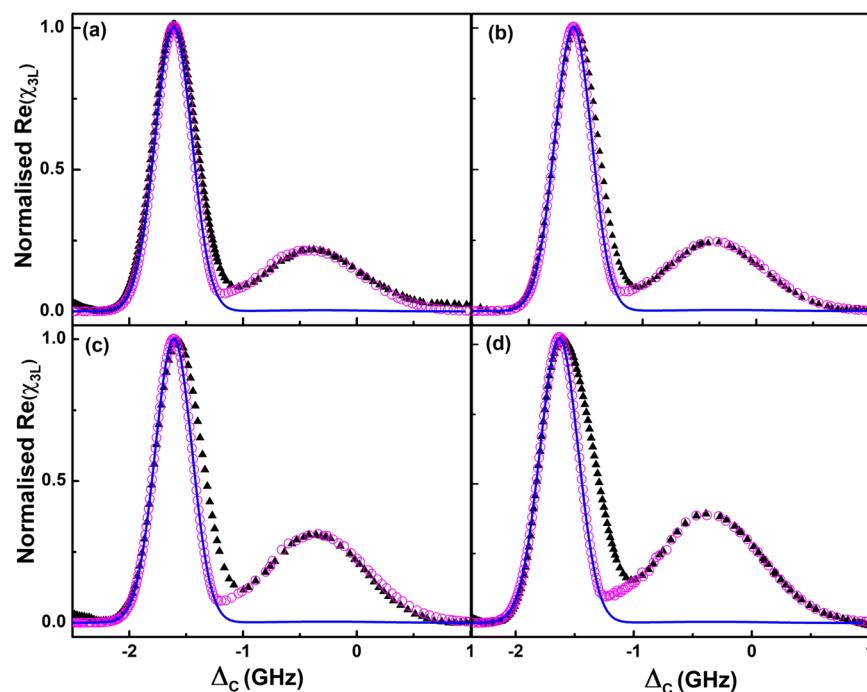


Figure 5. Dispersion spectrum measured from the experiment (black triangle) and calculated from the interacting two-atom model (open circle) for the Rydberg state with principal quantum numbers (a) $n=35$ (b) $n=40$ (c) $n=45$ and (d) $n=53$. For comparison, dispersion calculated from the non-interacting model is depicted as solid lines for all the n states.

The experiment was performed for the Rydberg states $35S_{1/2}$, $40S_{1/2}$, $45S_{1/2}$ and $53S_{1/2}$. The dispersion of the probe beam was measured using OHDT by varying the density of the rubidium vapor with laser parameters $\Omega_p = 400$ MHz, $\Omega_c = 4$ MHz and $\Delta_p = 1.25$ GHz. All the laser parameters including the gain in the set up were kept fixed throughout the experiment for all the Rydberg states. As predicted in the theoretical model, two different peaks were observed for the dispersion spectrum of the probe beam when the coupling laser is scanned over few GHz. One of them is the usual two photon resonant peak and the other one is the anti-blockade peak. Since the Rydberg-Rydberg interaction is repulsive, the anti-blockade peak is expected to be observed on the blue detuned side of the dispersion spectrum. For lower principal quantum number states the Rydberg interactions is weak and is significant only at very high atomic density. However, with increase in the principal

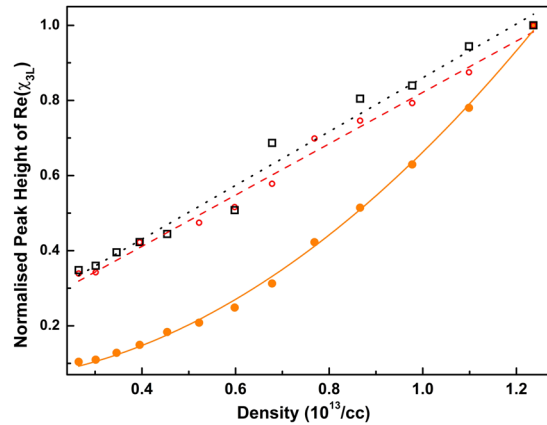


Figure 6. Anti-blockade peak height (solid circle) and the usual two-photon resonant peak height for $^{85}\text{Rb } 5S_{1/2}F=3 \rightarrow nS_{1/2}$ (open circle) and $^{85}\text{Rb } 5S_{1/2}F=2 \rightarrow nS_{1/2}$ transition (\diamond) for $n=35$ Rydberg state as a function of the density of the atomic vapor. The peak heights are normalized to the dispersion peak height corresponding to the highest density. Dotted lines are the straight line fitting of usual two-photon resonant peaks showing the linear dependence of density whereas the solid line is fitting of the anti-blockade peak height showing quadratic dependence of density.

quantum number of the Rydberg state, the interaction is significant and hence the anti-blockade peak is observed at lower densities as well. The width of the two photon resonant peak is nearly $\Delta k v_p$, while for the anti-blockade peak, it is about $k_C v_p$. The width of the anti-blockade peak is observed to be larger which seems to be in good agreement with the theoretical model as shown in Fig. 5. For repulsive interaction, as shown in Fig. 3(a), when the laser is red detuned, the contribution of the off resonant atom to the Rydberg population is less as compared to a blue detuned case. Referring to the two photon resonant peak, the anti-blockade effect is significantly larger on the blue detuned side compared to the red detuned side while coupling to $nS_{1/2}$ state. The two photon resonant peak contains both blockade and anti-blockade effect making it difficult to model. However, to have a qualitative understanding, this peak is compared to a non-interacting model. As shown in Fig. 5, with increase in principal quantum number, the experimental data deviates more from the non-interacting model. The deviation on the blue detuned side of the spectrum is an indication of the dominating anti-blockade effect.

For a fixed atomic density, the height of the anti-blockade peak increases with the principal quantum number of the Rydberg state. The C_6 scaling with the principal quantum number could not be determined from the anti-blockade peak observed in the experiment. When the number of atoms in the $|g_2\rangle$ state in the interaction sphere is more than one, the blockade effect will contribute along with the cascaded processes involving more number of atoms. For a Rydberg state with $n=35$, the interaction is small and the number of atoms in the $|g_2\rangle$ state in the interaction sphere, $N_b \approx 1$ at a density of $3.0 \times 10^{13}/\text{cc}$. Thus, the experimental data is expected to match well with the model. We measured the dispersion peak height for the anti-blockade peak and the two photon resonant peaks corresponding to the transitions $^{85}\text{Rb } 5S_{1/2}F=2 \rightarrow 35S_{1/2}$ and $^{85}\text{Rb } 5S_{1/2}F=3 \rightarrow 35S_{1/2}$ by varying the density of the vapor cell which is shown in Fig. 6. For $35S_{1/2}$, the anti-blockade peak height increases quadratically with increase in density as predicted in the model. For the other two peaks, the variation is observed to be linear. The peak corresponding to the transition $^{85}\text{Rb } 5S_{1/2}F=2 \rightarrow 35S_{1/2}$ is expected to be non-interacting as the applied laser is highly detuned from the atomic resonance resulting in linear dependence of density. For the two photon resonant peak corresponding to $^{85}\text{Rb } 5S_{1/2}F=3 \rightarrow 35S_{1/2}$, both the blockade and anti-blockade effects are present which may be compensating each other such that the variation with density is roughly linear. The dotted and dashed lines are the linear fittings and the solid line is the quadratic fit of the peak height data as shown in Fig. 6.

Conclusion

We have observed the interaction induced enhancement in Rydberg excitation in thermal rubidium vapor. A two atom interacting model is formulated using the dressed state picture of the three level atomic system to explain the anti-blockade peak. The population of the Rydberg state is observed to be enhancing quadratically with the density of the vapor for Rydberg state with $n=35$, as predicted in the theoretical model. The experiment performed here is limited by the uncertainty in the density measurement. The density dependence of the anti-blockade peak can be studied with a better measurement of density and larger number of data. The deviation from the quadratic behavior can be measured to study the effect of blockade and the cascaded processes on the anti-blockade peak having more than one atom in the $|g_2\rangle$ state in the interaction sphere.

Methods

Non-interacting dressed state model. The Hamiltonian for driving two atoms together is given by $H = H^{(1)} \otimes \mathbf{I} + \mathbf{I} \otimes H^{(2)}$, where $H^{(1)} = \frac{-\hbar}{2}(\Delta_1|g_1\rangle\langle g_1| + \Delta_1|r\rangle\langle r| + \Omega_1|g_1\rangle\langle r| + H.C.)$ and $H^{(2)} = \frac{-\hbar}{2}(\Delta_2|r\rangle\langle r| + \Omega_2|g_2\rangle\langle r| + H.C.)$ are the Hamiltonian for the individual atoms. The Lindblad operator for the two-

atom model can be written as $\mathcal{L}_D = \mathcal{L}_D^{(1)} \otimes \rho^{(2)} + \rho^{(1)} \otimes \mathcal{L}_D^{(2)}$, where $\mathcal{L}_D^{(j)} = \Gamma_j(C\rho^{(j)}C^\dagger - \frac{1}{2}(C^\dagger C\rho^{(j)} + \rho^{(j)}C^\dagger C) - \frac{\Gamma_{eg}}{2}(C^\dagger C\rho^{(j)}CC^\dagger + H.C.)$, where $j=1,2$ for atom 1 and atom 2 respectively and $C = |f\rangle\langle i|$, where $|i\rangle$ stands for the initial state from which the population decays to the final state $|f\rangle$ ⁴⁷. $\rho^{(1)}$ and $\rho^{(2)}$ represent the density matrices of atom 1 and 2 respectively. Rydberg population in the system can be determined from the steady state solution of the master equation $\dot{\rho} = \frac{1}{i\hbar}[H, \rho] + \mathcal{L}_D$. Rydberg population can be determined as $\rho_{rr} = \left(\frac{\rho_{22} + \rho_{33}}{2} + \rho_{44}\right) \frac{\Omega_p^4}{8\Delta_p^4}$ where the factor $\frac{\Omega_p^4}{8\Delta_p^4}$ is taken as the population of the state $|g_2, g_2\rangle$ including the normalization factor to account for

the population of the state $|g_2, g_1\rangle$. To model the system for thermal atomic vapor, both the atoms are considered to be moving with independent velocity v_l where l -index takes the value 1 or 2 depending on the atom being considered. For counter-propagating configuration of the probe and coupling lasers with wave vector k_p and k_c respectively, the detunings are modified as $\Delta_p = \Delta_p - k_p v_1$ and $\Delta_c = \Delta_c + k_c v_1$ with $\Delta k = k_c - k_p$. Thus the laser detunings from the two-atom transitions are modified as $\Delta_1 = \Delta_c + k_c v_1 - \Omega_p^2/4(\Delta_p - k_p v_1)$ and $\Delta_2 = \Delta_p + \Delta_c + (\Delta k)v_2 + \Omega_p^2/4(\Delta_p - k_p v_2)$. Doppler averaged Rydberg population can be determined by calculating the integral $\rho_{rr} = \frac{1}{\pi v_p^2} \iint \rho_{rr}(v_1, v_2) e^{-v_1^2/v_p^2} e^{-v_2^2/v_p^2} dv_1 dv_2$, with v_p being the most probable velocity. We have used a Monte-Carlo technique to evaluate the integral. The main peak at the two-photon resonance has to be calculated using the two-atom model by driving the atoms from the state $|g_2, g_2\rangle$ to the Rydberg state.

Interacting dressed state model. Referring to Fig. 3, consider that the atom in the dressed state $|g_1\rangle$ is placed at the center of the interaction sphere and the other atom in the dressed state $|g_2\rangle$ is present in a concentric spherical shell with radius r and thickness dr . Resonance condition to the $|rr\rangle$ state constrain the velocity of the second atom to depend on the velocity of first atom as well as on their inter-particle separation r . If the resonant atoms within the line width of Rabi coupling are assumed to contribute significantly to the anti-blockade then the above constraint can be used to reduce the complexity of the model. Taking the vapor density as η , the number of atoms in the dressed state $|g_2\rangle$ present inside the spherical shell with radius r is $\eta 4\pi r^2 dr$. Suppose, only the velocity class of atoms at v_2 within a small velocity width $\Delta v_2 = \Omega_2/\Delta k$ inside the same spherical shell satisfy the resonant condition to the $|rr\rangle$ state, then the effective number of atoms inside the interaction sphere contributing to the anti-blockade can be evaluated as $N_b(v_1) = \frac{4\pi\eta}{\sqrt{\pi} v_p} \frac{\Omega_2}{\Delta k} \int_0^{r_b} r^2 e^{-v_2^2/v_p^2} dr$ where v_2 depends on v_1 and r . In the case of probe laser detuning larger than the Doppler width, $\Delta_p \gg k_p v_2$, the light shift of the $|g_2\rangle$ state can be expanded to be $(1 + k_p v_2/\Delta_p) \Omega_p^2/4\Delta_p$, neglecting the higher order terms. Then, the velocity of the second atom is found to be $v_2 = (2C_6/r^6 - \Delta_1(v_1))/\Delta k'$, where $\Delta_1'(v_1) = \Delta_p + 2\Delta_c + k_c v_1 - \Omega_p^2 k_p v_1/4\Delta_p^2$ and $\Delta k' = \Delta k + \Omega_p^2 k_p/4\Delta_p^2$. The above integral can be solved analytically to find the total number of atoms contributing to the anti-blockade as $N_b(v_1) = \frac{\pi\eta\Omega_2\sqrt{8C_6\Delta k'}}{\Delta k(\Delta_1'(v_1))^{3/2}}$. Rydberg population can be related to the dispersion which is a measurable quantity

using optical heterodyne detection technique as $\Re(\chi_{3L}(v_1)) = \frac{\eta |\mu_{eg}|^2 N_b(v_1)}{\varepsilon_0 \hbar (\Delta_p - k_p v_1)} \rho_{rr}(v_1)$ ⁴². Averaging over the velocity distribution of the first atom, the dispersion of the probe due to anti-blockade can be evaluated as

$$\Re(\chi_{3L}) = \frac{\Omega_2 \sqrt{8\pi C_6} \Delta k' |\mu_{eg}|^2}{\varepsilon_0 \hbar v_p \Delta k} \eta^2 \int_{-\infty}^{\infty} \frac{\rho_{rr}(v_1) e^{-v_1^2/v_p^2}}{(\Delta_p - k_p v_1) (\Delta_1'(v_1))^{3/2}} dv_1 \quad (1)$$

References

- Saffman, M., Walker, T. G. & Mølmer, K. Quantum information with rydberg atoms. *Rev. Mod. Phys.* **82**, 2313–2363, <https://doi.org/10.1103/RevModPhys.82.2313> (2010).
- Dudin, Y. O., Li, L., Bariani, F. & Kuzmich, A. Observation of coherent many-body rabi oscillations. *Nat. Phys.* **8**, 790–794 (2012).
- Dudin, Y. O. & Kuzmich, A. Strongly interacting rydberg excitations of a cold atomic gas. *Science* **336**, 887–889 (2012).
- Tong, D. *et al.* Local blockade of rydberg excitation in an ultracold gas. *Phys. Rev. Lett.* **93**, 063001, <https://doi.org/10.1103/PhysRevLett.93.063001> (2004).
- Singer, K., Reetz-Lamour, M., Amthor, T., Marcassa, L. G. & Weidemüller, M. Suppression of excitation and spectral broadening induced by interactions in a cold gas of rydberg atoms. *Phys. Rev. Lett.* **93**, 163001, <https://doi.org/10.1103/PhysRevLett.93.163001> (2004).
- Liebisch, T. C., Reinhard, A., Berman, P. R. & Raithel, G. Atom counting statistics in ensembles of interacting rydberg atoms. *Phys. Rev. Lett.* **95**, 253002, <https://doi.org/10.1103/PhysRevLett.95.253002> (2005).
- Vogt, T. *et al.* Dipole blockade at Förster resonances in high resolution laser excitation of rydberg states of cesium atoms. *Phys. Rev. Lett.* **97**, 083003, <https://doi.org/10.1103/PhysRevLett.97.083003> (2006).
- Heidemann, R. *et al.* Evidence for coherent collective rydberg excitation in the strong blockade regime. *Phys. Rev. Lett.* **99**, 163601, <https://doi.org/10.1103/PhysRevLett.99.163601> (2007).
- Raitzsch, U. *et al.* Echo experiments in a strongly interacting rydberg gas. *Phys. Rev. Lett.* **100**, 013002, <https://doi.org/10.1103/PhysRevLett.100.013002> (2008).
- Urban, E. *et al.* Observation of rydberg blockade between two atoms. *Nature Phys.* **5**, 110–114 (2009).
- Gaëtan, A. *et al.* Observation of collective excitation of two individual atoms in the rydberg blockade regime. *Nat. Phys.* **5**, 115–118 (2009).
- Weimer, H., Löw, R., Pfau, T. & Büchler, H. P. Quantum critical behavior in strongly interacting rydberg gases. *Phys. Rev. Lett.* **101**, 250601, <https://doi.org/10.1103/PhysRevLett.101.250601> (2008).
- Pohl, T., Demler, E. & Lukin, M. D. Dynamical crystallization in the dipole blockade of ultracold atoms. *Phys. Rev. Lett.* **104**, 043002, <https://doi.org/10.1103/PhysRevLett.104.043002> (2010).
- Pupillo, G., Micheli, A., Boninsegni, M., Lesanovsky, I. & Zoller, P. Strongly correlated gases of rydberg-dressed atoms: Quantum and classical dynamics. *Phys. Rev. Lett.* **104**, 223002, <https://doi.org/10.1103/PhysRevLett.104.223002> (2010).
- Henkel, N., Nath, R. & Pohl, T. Three-dimensional roton excitations and supersolid formation in rydberg-excited bose-einstein condensates. *Phys. Rev. Lett.* **104**, 195302, <https://doi.org/10.1103/PhysRevLett.104.195302> (2010).

16. Busche, H. *et al.* Contactless nonlinear optics mediated by long-range rydberg interactions. *Nature Phys.* **13**, 655–658 (2017).
17. Peyronel, T. *et al.* Quantum nonlinear optics with single photons enabled by strongly interacting atoms. *Nat.* **488**, 57–60 (2012).
18. Firstenberg, O. *et al.* Attractive photons in a quantum nonlinear medium. *Nature* **502**, 71–75 (2013).
19. Jaksch, D. *et al.* Fast quantum gates for neutral atoms. *Phys. Rev. Lett.* **85**, 2208–2211, <https://doi.org/10.1103/PhysRevLett.85.2208> (2000).
20. Isenhower, L. *et al.* Demonstration of a neutral atom controlled-not quantum gate. *Phys. Rev. Lett.* **104**, 010503, <https://doi.org/10.1103/PhysRevLett.104.010503> (2010).
21. Wilk, T. *et al.* Entanglement of two individual neutral atoms using rydberg blockade. *Phys. Rev. Lett.* **104**, 010502 (2010).
22. Lukin, M. D. *et al.* Dipole blockade and quantum information processing in mesoscopic atomic ensembles. *Phys. Rev. Lett.* **87**, 037901, <https://doi.org/10.1103/PhysRevLett.87.037901> (2001).
23. Ates, C., Pohl, T., Pattard, T. & Rost, J. M. Antiblockade in rydberg excitation of an ultracold lattice gas. *Phys. Rev. Lett.* **98**, 023002, <https://doi.org/10.1103/PhysRevLett.98.023002> (2007).
24. Amthor, T., Giese, C., Hofmann, C. S. & Weidemüller, M. Evidence of antiblockade in an ultracold rydberg gas. *Phys. Rev. Lett.* **104**, 013001, <https://doi.org/10.1103/PhysRevLett.104.013001> (2010).
25. Pohl, T. & Berman, P. R. Breaking the dipole blockade: Nearly resonant dipole interactions in few-atom systems. *Phys. Rev. Lett.* **102**, 013004, <https://doi.org/10.1103/PhysRevLett.102.013004> (2009).
26. Qian, J. *et al.* Breakdown of the dipole blockade with a zero-area phase-jump pulse. *Phys. Rev. A* **80**, 053413, <https://doi.org/10.1103/PhysRevA.80.053413> (2009).
27. Weber, T. M. *et al.* Mesoscopic rydberg-blockaded ensembles in the superatom regime and beyond. *Nat. Phys.* **11**, 157–161, <https://doi.org/10.1038/nphys3214> (2015).
28. Goldschmidt, E. A. *et al.* Anomalous broadening in driven dissipative rydberg systems. *Phys. Rev. Lett.* **116**, 113001, <https://doi.org/10.1103/PhysRevLett.116.113001> (2016).
29. Letscher, F., Thomas, O., Niederprüm, T., Fleischhauer, M. & Ott, H. Bistability versus metastability in driven dissipative rydberg gases. *Phys. Rev. X* **7**, 021020, <https://doi.org/10.1103/PhysRevX.7.021020> (2017).
30. Derevianko, A., Kómar, P., Topcu, T., Kroeze, R. M. & Lukin, M. D. Effects of molecular resonances on rydberg blockade. *Phys. Rev. A* **92**, 063419, <https://doi.org/10.1103/PhysRevA.92.063419> (2015).
31. Sárkány, Lm. H., Fortágh, J. & Petrosyan, D. Long-range quantum gate via rydberg states of atoms in a thermal microwave cavity. *Phys. Rev. A* **92**, 030303, <https://doi.org/10.1103/PhysRevA.92.030303> (2015).
32. Su, S.-L. *et al.* One-step implementation of the rydberg-rydberg-interaction gate. *Phys. Rev. A* **93**, 012306, <https://doi.org/10.1103/PhysRevA.93.012306> (2016).
33. Su, S.-L., Gao, Y., Liang, E. & Zhang, S. Fast rydberg antiblockade regime and its applications in quantum logic gates. *Phys. Rev. A* **95**, 022319, <https://doi.org/10.1103/PhysRevA.95.022319> (2017).
34. Baluktian, T., Huber, B., Löw, R. & Pfau, T. Evidence for strong van der waals type rydberg-rydberg interaction in a thermal vapor. *Phys. Rev. Lett.* **110**, 123001, <https://doi.org/10.1103/PhysRevLett.110.123001> (2013).
35. Urvoy, A. *et al.* Strongly correlated growth of rydberg aggregates in a vapor cell. *Phys. Rev. Lett.* **114**, 203002, <https://doi.org/10.1103/PhysRevLett.114.203002> (2015).
36. Carr, C., Ritter, R., Wade, C. G., Adams, C. S. & Weatherill, K. J. Nonequilibrium phase transition in a dilute rydberg ensemble. *Phys. Rev. Lett.* **111**, 113901, <https://doi.org/10.1103/PhysRevLett.111.113901> (2013).
37. Mohapatra, A. K., Bason, M. G., Butscher, B., Weatherill, K. J. & Adams, C. S. A giant electro-optic effect using polarizable dark states. *Nature Phys.* **4**, 890–894 (2008).
38. de Melo, N. R. *et al.* Intrinsic optical bistability in a strongly driven rydberg ensemble. *Phys. Rev. A* **93**, 063863, <https://doi.org/10.1103/PhysRevA.93.063863> (2016).
39. Mohapatra, A. K., Jackson, T. R. & Adams, C. S. Coherent optical detection of highly excited rydberg states using electromagnetically induced transparency. *Phys. Rev. Lett.* **98**, 113003, <https://doi.org/10.1103/PhysRevLett.98.113003> (2007).
40. Kübler, H., Shaffer, J. P., Baluktian, T., Löw, R. & Pfau, T. Coherent excitation of rydberg atoms in micrometre-sized atomic vapour cells. *Nature Phot.* **4**, 112–116 (2010).
41. Kölle, A., Epple, G., Kübler, H., Löw, R. & Pfau, T. Four-wave mixing involving rydberg states in thermal vapor. *Phys. Rev. A* **85**, 063821, <https://doi.org/10.1103/PhysRevA.85.063821> (2012).
42. Bhowmick, A., Sahoo, S. S. & Mohapatra, A. K. Optical nonlinearity of rydberg electromagnetically induced transparency in thermal vapor using the optical-heterodyne-detection technique. *Phys. Rev. A* **94**, 023839, <https://doi.org/10.1103/PhysRevA.94.023839> (2016).
43. Bhowmick, A., Kara, D. & Mohapatra, A. K. Study of Rydberg blockade in thermal vapor. arXiv:1802.06599v1 (2018).
44. Letscher, F., Thomas, O., Niederprüm, T., Ott, H. & Fleischhauer, M. Anomalous excitation facilitation in inhomogeneously broadened rydberg gases. *Phys. Rev. A* **95**, 023410, <https://doi.org/10.1103/PhysRevA.95.023410> (2017).
45. Bhowmick, A., Kara, D. & Mohapatra, A. K. Study of rydberg blockade mediated optical non-linearity in thermal vapor using optical heterodyne detection technique. arXiv:1605.06603 (2016).
46. Han, R., Khoon, N., H. & Englert, B.-G. Raman transitions without adiabatic elimination: a simple and accurate treatment. *Journal of Modern Optics* **60**, 255–265, <https://doi.org/10.1080/09500340.2013.770573> (2013).
47. Béguin, L., Vernier, A., Chicireanu, R., Lahaye, T. & Browaeys, A. Direct measurement of the van der waals interaction between two rydberg atoms. *Phys. Rev. Lett.* **110**, 263201, <https://doi.org/10.1103/PhysRevLett.110.263201> (2013).

Acknowledgements

We would like to thank Dr. V. Ravi Chandra and Dr. Anamitra Mukherjee for their valuable suggestion for the theoretical modeling. We would like to thank Sushree S. Sahoo, Snigdha S. Pati and Tanim Firdoshi for assisting in performing the experiment. This experiment is financially supported by Department of Atomic Energy, Government of India.

Author Contributions

A.K.M. conceived the concept of anti-blockade in thermal vapor. A.K.M. and D.K. contributed to the theoretical modeling. D.K., A.B. and A.K.M. contributed in performing the experiment. D.K. analyzed the experimental data. All authors have contributed to the manuscript preparation.

Additional Information

Competing Interests: The authors declare no competing interests.

Publisher's note: Springer Nature remains neutral with regard to jurisdictional claims in published maps and institutional affiliations.



Open Access This article is licensed under a Creative Commons Attribution 4.0 International License, which permits use, sharing, adaptation, distribution and reproduction in any medium or format, as long as you give appropriate credit to the original author(s) and the source, provide a link to the Creative Commons license, and indicate if changes were made. The images or other third party material in this article are included in the article's Creative Commons license, unless indicated otherwise in a credit line to the material. If material is not included in the article's Creative Commons license and your intended use is not permitted by statutory regulation or exceeds the permitted use, you will need to obtain permission directly from the copyright holder. To view a copy of this license, visit <http://creativecommons.org/licenses/by/4.0/>.

© The Author(s) 2018